Geodesic Finite Elements for Cosserat Rods

Oliver Sander

June 8, 2009

Abstract

We introduce geodesic finite elements as a new way to discretize the nonlinear configuration space of a geometrically exact Cosserat rod. These geodesic finite elements naturally generalize standard one-dimensional finite elements to spaces of functions with values in a Riemannian manifold. For the special orthogonal group, our approach reproduces the interpolation formulas of Crisfield and Jelenić [6]. Geodesic finite elements are conforming and lead to objective and path-independent problem formulations. We introduce geodesic finite elements for general Riemannian manifolds, discuss the relationship between geodesic finite elements and coefficient vectors, and estimate the interpolation error. Then we use them to find static equilibria of hyperelastic Cosserat rods. Using the Riemannian trust-region algorithm of Absil et al. [1] we show numerically that the discretization error depends optimally on the mesh size.

1 Introduction

Cosserat rods are a standard model for the simulation of long slender structures. They are geometrically exact, meaning that the strains are not assumed to be small, and support tension and shear motion, as well as torsion and bending. There is a wide range of possible constitutive laws, and not only elastic, but also viscous and plastic material behavior can be modelled. Cosserat rods have found many applications, mainly in structural mechanics and computer graphics.

Mathematically, a Cosserat rod configuration is a function

$$\varphi : [0, l] \to \mathrm{SE}(3),$$

where $l > 0$ is the rod reference length, and

$$\mathrm{SE}(3) = \mathbb{R}^3 \rtimes \mathrm{SO}(3)$$

is the group of rigid-body motions in $\mathbb{R}^3$ (the special Euclidean group). For each $s \in [0, l]$, the value $\varphi(s) \in \mathrm{SE}(3)$ is interpreted as the position and orientation of the rigid cross-section of the rod at s. If the material law is hyperelastic, equilibrium configurations can be characterized as being stationary values of an energy functional

$$j(\varphi) = \int_{[0,l]} W(\varphi(s), \varphi'(s))\, ds \tag{1}$$

for some energy density function $W : T\mathrm{SE}(3) \to \mathbb{R}$.

The nonlinearity of the rod configuration space prohibits the use of standard discretization techniques. The standard approach of the linear finite element method would be to restrict the minimization of (1) to a finite-dimensional space, usually a subspace of the continuous one. The finite-dimensional space is constructed by setting up a grid $\mathcal{G}$, which, in the case of a one-dimensional domain $\Omega = [0, l]$ is a partitioning of $[0, l]$ in a set of nonoverlapping intervals

$$[0, l] = \prod_{i=0}^{n-2} [l_i, l_{i+1}]. \tag{2}$$

The discrete functions are then constructed from coefficient vectors and certain interpolation rules. In the easiest case the coefficients correspond to function values at the grid vertices and the discrete functions are defined by piecewise linear interpolation.

While this works well as long as φ takes values in a linear space, it is unclear how the construction can be generalized to nonlinear spaces. Linear interpolation depends on the presence of a vector space structure, and the one-to-one correspondence between discrete functions and vectors of coefficients implicitly assumes the presence of a basis of the ansatz space, which is also only available in vector spaces. Stated in more practical terms, it is unclear how to interpolate between two given coefficients $v_i, v_{i+1} \in \mathrm{SE}(3)$. For a given element $[l_i, l_{i+1}]$, the integral (1) needs to be approximated by a quadrature formula,

$$\int_{[l_i, l_{i+1}]} W(\varphi(s), \varphi'(s))\, ds \approx \sum_j w_j W(\varphi(q_j), \varphi'(q_j))$$

with $q_j \in [l_i, l_{i+1}]$ a finite set of quadrature points and $w_j \in \mathbb{R}$ the corresponding weights. The standard (first-order) finite element method defines $\varphi(q_j)$ and $\varphi'(q_j)$ by linear interpolation between v_i and v_{i+1}. However, this is not possible for rod problems because SE(3) is nonlinear.

This problem has been widely discussed in the literature, and several approaches have been proposed. Simo and Vu-Quoc [16] suggested to never interpolate rotations but to treat the values $\varphi(q_j)$ and gradients $\varphi'(q_j)$ at the quadrature points as history variables. Each iteration step of a Newton-type solver would produce a vector of corrections $c \in T\mathrm{SE}(3)^n$. Since each tangent space of $\mathrm{SE}(3)^n$ is linear, the algebraic corrections could be associated to linear finite element functions, and hence updates for the values at the quadrature points could be computed.

The method by Simo and Vu-Quoc was widely used until, however, Crisfield and Jelenić [6] showed that the outcome is path-dependent, even if the original problem is not. To interpolate on the rotation group SO(3) they suggested instead to consider the finite rotation from v_i to v_{i+1} and interpolate the rotation angle. This is path-independent, as only total rotational parameters are interpolated and no incremental ones (cf. [14, p. 14]). Crisfield and Jelenić also proved that their interpolation method is objective, meaning that the strain measures are invariant under rigid-body movements of the observer.

Sansour and Wagner [14] proposed another interpolation method that is also path-independent. They used the inverse exponential map on SO(3) to map nodal values onto the Lie algebra $\mathfrak{so}(3)$, which is the space of skew-symmetric matrices. This being a linear space, intermediate values could be computed there

and mapped back onto SO(3). Crisfield and Jelenić [6] also showed, however, that this interpolation method cannot be objective.

In this work we solve the interpolation problem for all spaces of functions from an interval $[0, l]$ to a Riemannian manifold M. In the case of $M = \mathrm{SE}(3)$, the interpolation formulas of Crisfield and Jelenić [6] are recovered. Since no incremental parameters are interpolated the formulation is path-independent, and we prove objectivity for arbitrary M. We also prove optimality of the interpolation error, which is a first step towards discretization error bounds for the discretization of Cosserat rod problems. To our knowledge, this question has not previously been given attention. We present numerical evidence that suggests that the discretization error of geodesic finite elements behaves optimally.

To solve the algebraic optimization problems on the nonlinear space $\mathrm{SE}(3)^n$, previous approaches used a Newton-type method for the first-order optimality condition $\nabla j = 0$ (see, e.g., [16]). The global convergence behavior of this is uncertain. In their monograph [1], Absil et al. worked out a theory for trust-region algorithms for optimization problems on matrix manifolds. We show how these solvers can be used to solve Cosserat rod problems to obtain a globally convergent, locally quadratic algorithm.

This article is structured as follows. In Chapter 2 we recall a few notions from Riemannian geometry and fix our notation. Chapter 3 formally defines Cosserat rods. The central Chapter 4 then introduces geodesic finite elements as an intrinsic way to discretize problems involving functions mapping an interval to a Riemannian manifold. We discuss the relationship of geodesic finite element functions to coefficient vectors, prove objectivity of the interpolation, and show that the interpolation error is optimal. In Chapter 5 we work out geodesic finite elements specifically for problems with values in SE(3). Using quaternion coordinates the interpolation formulas can be given explicitly. Chapter 6 then briefly introduces Riemannian trust-region algorithms and shows how they can be used to solve Cosserat rod problems. The final Chapter 7 gives two numerical examples. The first demonstrates the performance of the solver, whereas the second measures the discretization error in several norms and shows that is does indeed behave optimally.

2 Geometric Preliminaries

Riemannian Geometry Let M be a differentiable manifold with a Riemannian metric g and let $c : [a, b] \to M$ be a curve on M. For each $t \in [a, b]$ denote by $c'(t) \in T_{c(t)}M$ the velocity vector. The length of the curve is given by $\mathcal{L}(c) = \int_{[a,b]} \|c'(t)\|_g \, ds$. A curve c is called a *geodesic* if $\|c'\|_g$ is constant and if c minimizes $\mathcal{L}$ locally. This means that for all $\bar{a} < \bar{b}$, $\bar{a}, \bar{b} \in [a, b]$ and $\bar{b} - \bar{a}$ small enough the curve c restricted to $[\bar{a}, \bar{b}]$ is the shortest curve from $c(\bar{a})$ to $c(\bar{b})$ on M. Intuitively, geodesics generalize the notion of straight lines. We write

$$\gamma_M[p, q](\cdot) : [0, 1] \to M$$

to denote a minimizing geodesic on M from p to q with the parameter domain $[0, 1]$.

Let $q \in M$ and $v \in T_qM$. Then there is an interval I about 0 and a unique geodesic $\kappa : I \to M$ such that $\kappa(0) = q$ and $\kappa'(0) = v$. The mapping

$$\exp_q : U \subset T_qM \to M, \qquad \exp_q v = \kappa(1), \tag{3}$$

is called the *exponential map*. It maps a neighborhood U of $0 \in T_qM$ onto a neighborhood of q in M. From the implicit function theorem it follows that the exponential map is C^∞ on a neighborhood of $0 \in T_qM$ [8, Prop. 3.2.9]. Locally, the curves of the form $c : [-\epsilon, \epsilon] \to M$, $c(t) = \exp_q tv$ for $q \in M$, $v \in T_qM$ are geodesics, and all geodesics can be written in this way. A manifold M is called *(geodesically) complete* if for each pair $p, q \in M$ there exists at least one geodesic that joins p with q. Geodesically complete manifolds are metric spaces where the distance $\operatorname{dist}(p, q)$ between two points $p, q \in M$ is given by the length of the shortest geodesic between p and q. We have the following important result [8, Lem. 3.3.7].

Lemma 2.1. *For any $p \in M$ there exists an open neighborhood W of p such that $\operatorname{dist}(p, \cdot) : W \to \mathbb{R}$ depends differentiably on its second argument.*

If M and N are two manifolds, their Cartesian product $M \times N$ consisting of tuples (p, q) with $p \in M, q \in N$ is again a manifold. The tangent spaces have the structure

$$T_{(p,q)}(M \times N) = T_pM \oplus T_qN,$$

where $\oplus$ denotes the direct sum of vector spaces. If M and N are equipped with Riemannian metrics g and h, respectively, the product manifold can be turned into a Riemannian manifold by using the metric $\hat{g}_{(p,q)} = g_p + h_q$. The product $M \times N$ is complete if both M and N are. If $(p, q) \in M \times N$ and $(v, w) \in T_{(p,q)}(M \times N)$, then

$$\exp_{(p,q)}(v, w) = (\exp_p v, \exp_q w), \tag{4}$$

for all $v \in T_pM$, $w \in T_qN$ such that the right-hand side is defined. Construction of k-fold Cartesian product manifolds is done by induction.

The Special Orthogonal Group SO(3) A *Lie group* is a manifold G that has a group structure consistent with its manifold structure in the sense that group multiplication

$$\chi : G \times G \to G, \quad (g, h) \to gh,$$

is a C^∞ map. The tangent space T_eG at the identity e of G is called its *Lie algebra* and denoted by $\mathfrak{g}$.

An important Lie group is the group of rotations in $\mathbb{R}^3$, commonly denoted by SO(3). It can be represented by the set of all 3×3 matrices Q with $Q^TQ = \mathrm{Id}$ and $\det Q = 1$. As a manifold, SO(3) is three-dimensional and compactly embedded in the Euclidean space $\mathbb{R}^{3\times3}$ of all 3×3 matrices. Using this compactness of SO(3) and the theorem of Hopf and Rinow [8, Thm. 7.2.8] the following lemma can be shown.

Lemma 2.2. *SO(3) is geodesically complete.*

We have the following characterization of the tangent spaces of SO(3).

Lemma 2.3. *Let $\mathbb{A}^3$ be the space of antisymmetric 3×3 matrices and let $p \in SO(3)$. Then*

$$T_pSO(3) = p\mathbb{A}^3 := \{m \in \mathbb{R}^{3\times3} \mid m = p\hat{v},\ \hat{v} \in \mathbb{A}^3\}. \tag{5}$$

See [13] for a proof. In view of this lemma we will frequently write $p\hat{v}$, with $\hat{v} \in \mathbb{A}^3$, to denote an element of $p\mathbb{A}^3$. From Lemma 2.3 follows in particular that the Lie algebra $\mathfrak{so}(3)$ of $\mathrm{SO}(3)$ is the vector space $\mathbb{A}^3$ of antisymmetric 3×3 matrices. We may identify $\mathfrak{so}(3)$ with $\mathbb{R}^3$ via the *hat map* $\hat{}: \mathbb{R}^3 \to \mathfrak{so}(3)$ setting

$$v = (v_1, v_2, v_3) \to \hat{v} = \begin{pmatrix} 0 & -v_3 & v_2 \\ v_3 & 0 & -v_1 \\ -v_2 & v_1 & 0 \end{pmatrix}. \tag{6}$$

The canonical Euclidean metric $g(A, B) = \mathrm{tr}(A^T B)$ of $\mathbb{R}^{3\times 3}$ induces on $\mathrm{SO}(3)$ the metric

$$g_q(q\hat{v}_1, q\hat{v}_2) = \mathrm{tr}(\hat{v}_1^T \hat{v}_2) = \langle v_1, v_2 \rangle, \qquad q \in \mathrm{SO}(3),$$

see [1]. Using a general result about Lie group homomorphisms [17, Chap. 10, Prop. 9], the exponential map can be written as

$$\exp_q q\hat{v} = q \exp \hat{v}, \tag{7}$$

where exp (without the subscript) is used to denote the exponential map of $\mathrm{SO}(3)$ at the identity. A corresponding result holds for all Lie groups.

The Special Euclidean Group SE(3) The special Euclidean group $\mathrm{SE}(3)$ is the semi-direct product

$$\mathrm{SE}(3) = \mathbb{R}^3 \rtimes \mathrm{SO}(3),$$

which is the group of rigid-body transformations of $\mathbb{R}^3$. As a manifold, $\mathrm{SE}(3)$ is equal to the Cartesian product $\mathbb{R}^3 \times \mathrm{SO}(3)$. We will denote elements of $\mathrm{SE}(3)$ by tuples (r, q) with $r \in \mathbb{R}^3$ and $q \in \mathrm{SO}(3)$. Using the rule for product manifolds (4) given above, the exponential map on $\mathrm{SE}(3)$ is given by

$$\exp_{(r,q)}(w, q\hat{v}) = (r + w, q \exp \hat{v}),$$

where we have used that $\exp_r w = r + w$ in vector spaces.

Unit Quaternions as Coordinates on SO(3) For computations on $\mathrm{SO}(3)$ the *unit quaternions* $\mathbb{H}_{|1|}$ form a set of suitable coordinates. Quaternions are quadruples of real numbers $q = (q_1, q_2, q_3, q_4)$. Together with the multiplication $p = q\tilde{q}$,

$$\begin{aligned} p_1 &= q_4\tilde{q}_1 - q_3\tilde{q}_2 + q_2\tilde{q}_3 + q_1\tilde{q}_4, \\ p_2 &= q_3\tilde{q}_1 + q_4\tilde{q}_2 - q_1\tilde{q}_3 + q_2\tilde{q}_4, \\ p_3 &= -q_2\tilde{q}_1 + q_1\tilde{q}_2 + q_4\tilde{q}_3 + q_3\tilde{q}_4, \\ p_4 &= -q_1\tilde{q}_1 - q_2\tilde{q}_2 - q_3\tilde{q}_3 + q_4\tilde{q}_4, \end{aligned}$$

they form a noncommutative algebra $\mathbb{H}$. In this algebra, the inverse element can be expressed as

$$q^{-1} = \frac{\bar{q}}{|q|^2},$$

where $\bar{q} = (-q_1, -q_2, -q_3, q_4)$ is the element *conjugate* to q and $|q| = \sqrt{\sum_i q_i^2}$ is the absolute value. The unit quaternions $\mathbb{H}_{|1|}$ are the subset of $\mathbb{H}$ for which

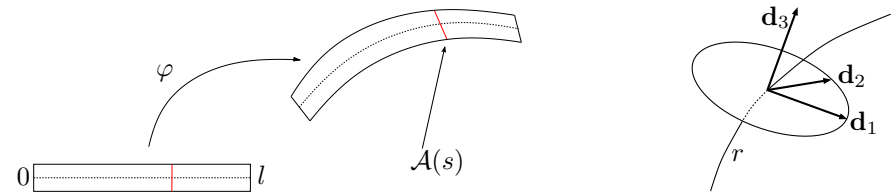

Figure 1: Kinematics of Cosserat rods. Left: under deformation, rod cross-sections remain planar, but not necessarily orthogonal to the centerline. Right: the cross-section orientation is represented by three orthonormal director vectors.

$|q| = 1$. They form a double covering of SO(3), meaning that there exists a smooth two-to-one mapping from $\mathbb{H}_{|1|}$ onto SO(3) which maps the multiplication in $\mathbb{H}$ onto the group multiplication in SO(3). Therefore, unit quaternions are convenient as global coordinates on SO(3). We would like to stress, though, that the discretization we propose in Chapter 4 is independent of the coordinates used.

In quaternion coordinates there is a closed-form expression for the exponential map of SO(3). Let $\hat{v} \in \mathbb{A}^3 = \mathfrak{so}(3)$ and let $v = (v_1, v_2, v_3)$ be the vector corresponding to $\hat{v}$ by the hat map (6). Then $q = \exp \hat{v} \in \mathbb{H}_{|1|}$ is given by

$$q_j = \frac{v_j}{|v|} \sin \frac{|v|}{2} \quad \text{for } j = 1, 2, 3, \qquad \text{and} \qquad q_4 = \cos \frac{|v|}{2}, \tag{8}$$

(see [7]). Setting $\exp 0 = (0, 0, 0, 1)$ the function exp is C^∞ at 0 as expected from the general theory.

3 Cosserat Rods

In this section we briefly present Cosserat rods, which model the large deformation behavior of long, slender objects. For an in-depth presentation see the book by Antman [2].

Kinematics Configurations of Cosserat rods are maps

$$\begin{aligned} \varphi : [0, l] &\rightarrow \mathrm{SE}(3) \\ s &\rightarrow (r, q), \end{aligned}$$

for some $l > 0$. While the first component $r \in \mathbb{R}^3$ of φ determines the position of the *centerline* of the rod at s, the second component $q \in \mathrm{SO}(3)$ determines the orientation of an idealized rigid cross-section $\mathcal{A}(s)$ (Fig. 1, left). This orientation is commonly represented by three pairwise orthonormal vectors $\mathbf{d}_1, \mathbf{d}_2, \mathbf{d}_3 \in \mathbb{R}^3$, which are called *directors* (Fig. 1, right). When quaternions are used as

coordinates on SO(3), the expressions for the three directors are

$$\begin{aligned}
\mathbf{d}_1(q) &= \begin{pmatrix} q_1^2 - q_2^2 - q_3^2 + q_4^2 \\ 2(q_1q_2 + q_3q_4) \\ 2(q_1q_3 - q_2q_4) \end{pmatrix}, \\
\mathbf{d}_2(q) &= \begin{pmatrix} 2(q_1q_2 - q_3q_4) \\ -q_1^2 + q_2^2 - q_3^2 + q_4^2 \\ 2(q_2q_3 + q_1q_4) \end{pmatrix}, \\
\mathbf{d}_3(q) &= \begin{pmatrix} 2(q_1q_3 + q_2q_4) \\ 2(q_2q_3 - q_1q_4) \\ -q_1^2 - q_2^2 + q_3^2 + q_4^2 \end{pmatrix}.
\end{aligned}$$

Rod strains are described by two functions $\mathbf{v}, \mathbf{u} : [0, l] \to \mathbb{R}^3$ which are defined by the relations

$$\mathbf{v}(s) = r'(s), \qquad s \in [0, l],$$

and

$$\mathbf{d}_k'(s) = \mathbf{u}(s) \times \mathbf{d}_k(s), \qquad k = 1, 2, 3, \qquad s \in [0, l],$$

where the prime denotes derivation with respect to s. In order to make these strain measures invariant under rigid-body motions they are expressed in the local coordinate systems spanned by the directors $\mathbf{d}_k$. We introduce the new vectors

$$\mathsf{v} = (\mathsf{v}_1, \mathsf{v}_2, \mathsf{v}_3) = \big(\langle \mathbf{v}, \mathbf{d}_1 \rangle, \langle \mathbf{v}, \mathbf{d}_2 \rangle, \langle \mathbf{v}, \mathbf{d}_3 \rangle\big)$$

and

$$\mathsf{u} = (\mathsf{u}_1, \mathsf{u}_2, \mathsf{u}_3) = \big(\langle \mathbf{u}, \mathbf{d}_1 \rangle, \langle \mathbf{u}, \mathbf{d}_2 \rangle, \langle \mathbf{u}, \mathbf{d}_3 \rangle\big).$$

In the context of rod mechanics we will always use sans serif characters to denote quantities in coordinates of the director frame. The components v_1 and v_2 are interpreted as the shear strains, while v_3 is the stretching strain. The components u_1 and u_2 are the bending strains, and u_3 the strain related to torsion. Using quaternion coordinates the components u_k can be written as

$$\mathsf{u}_k = 2\mathbf{B}_k(q)q',$$

where the linear mappings $\mathbf{B}_k : \mathbb{H} \to \mathbb{H}$ are defined as

$$\begin{aligned}
\mathbf{B}_1 q &= (q_4, q_3, -q_2, -q_1), \\
\mathbf{B}_2 q &= (-q_3, q_4, q_1, -q_2), \\
\mathbf{B}_3 q &= (q_2, -q_1, q_4, -q_3).
\end{aligned}$$

These mappings can be interpreted such that for small $\epsilon \in \mathbb{R}$, a change in q by $\epsilon\mathbf{B}_k(q)$ produces a rotation about the $\mathbf{d}_k$ axis by an angle of 2ϵ [7].

For a meaningful theory deformations have to preserve the orientation of the material. In particular it should be impossible to compress any part of a rod with positive rest length to zero length. The simplest condition is

$$\mathsf{v}_3 = \langle \mathbf{v}, \mathbf{d}_3 \rangle > 0. \tag{9}$$

A more involved treatment which takes the finite cross-sectional area of the rod into account is given by Antman [2].

Forces and Moments The forces and moments acting across a cross-section $\mathcal{A}(s)$, $s \in [0,l]$ are implicitly averaged to yield a resultant force $\mathbf{n}(s) \in \mathbb{R}^3$ and a resultant moment $\mathbf{m}(s) \in \mathbb{R}^3$ about $r(s) \in \mathbb{R}^3$. Then balance of forces and moments implies the equilibrium equations

$$\begin{aligned} \mathbf{n}' + \mathbf{f} &= 0, \qquad \text{on } [0,l], \qquad (10) \\ \mathbf{m}' + r' \times \mathbf{n} + \mathbf{l} &= 0, \qquad \text{on } [0,l], \qquad (11) \end{aligned}$$

where $\mathbf{f} : [0,l] \to \mathbb{R}^3$ is an external force and $\mathbf{l} : [0,l] \to \mathbb{R}^3$ an external moment [2]. The components of the net forces $\mathbf{n}$ and moments $\mathbf{m}$ with respect to the local coordinate systems spanned by the directors are denoted n_i and m_i, $i \in \{1,2,3\}$, respectively. We refer to m_1, m_2 as the bending moments and to m_3 as the twisting moment. The components n_1 and n_2 are the shear forces and n_3 the tension.

Constitutive Laws Forces and moments are linked to the strain by constitutive relations which describe the properties of specific materials. A material is called *hyperelastic* if there exists an energy functional $W(\mathsf{w},\mathsf{z})$ with $\mathsf{w} = (\mathsf{w}_1, \mathsf{w}_2, \mathsf{w}_3)$, $\mathsf{z} = (\mathsf{z}_1, \mathsf{z}_2, \mathsf{z}_3)$ such that

$$\mathsf{m} = \frac{\partial W}{\partial \mathsf{w}}(\mathsf{u} - \hat{\mathsf{u}}, \mathsf{v} - \hat{\mathsf{v}}), \quad \text{and} \quad \mathsf{n} = \frac{\partial W}{\partial \mathsf{z}}(\mathsf{u} - \hat{\mathsf{u}}, \mathsf{v} - \hat{\mathsf{v}}). \qquad (12)$$

Here, $\hat{\mathsf{u}}$ and $\hat{\mathsf{v}}$ are the components of strain in a reference configuration $\hat{\varphi} : [0,l] \to \mathrm{SE}(3)$. We assume this reference configuration to be stress-free by requiring that

$$\frac{\partial W}{\partial \mathsf{w}}(0,0) = \frac{\partial W}{\partial \mathsf{z}}(0,0) = 0.$$

Further we take the strain-energy function W to be convex, coercive, and as smooth as needed by the analysis. Recall that the function W is called *coercive* if

$$\frac{W(\mathsf{w},\mathsf{z})}{\sqrt{|\mathsf{w}|^2 + |\mathsf{z}|^2}} \to \infty \quad \text{as} \quad |\mathsf{w}|^2 + |\mathsf{z}|^2 \to \infty$$

(see [2, 9]).

Formulation as a Minimization Problem As with other hyperelastic models, the stable equilibrium configurations of a Cosserat rod with a hyperelastic material law can be characterized as the minima of an energy functional. For this, let M be a Riemannian manifold and recall the definition of the Sobolev space $W^{1,p}([0,l],M)$ given in [3]. By the Nash embedding theorem, M can be isometrically embedded in $\mathbb{R}^k$ for some $k \geq 1$ [11]. This allows to define $W^{1,p}([0,l],M)$ by

$$W^{1,p}([0,l],M) = \big\{ v \in W^{1,p}([0,l],\mathbb{R}^k) \mid v(x) \in M \text{ a.e.} \big\}. \qquad (13)$$

Introduce the energy functional

$$\begin{aligned} j &: W^{1,p}([0,l],\mathrm{SE}(3)) \to \mathbb{R} \\ j(\varphi) &= \int_{[0,l]} W\big(\mathsf{u}(\varphi) - \hat{\mathsf{u}}, \mathsf{v}(\varphi) - \hat{\mathsf{v}}\big)\, ds \qquad (14) \end{aligned}$$

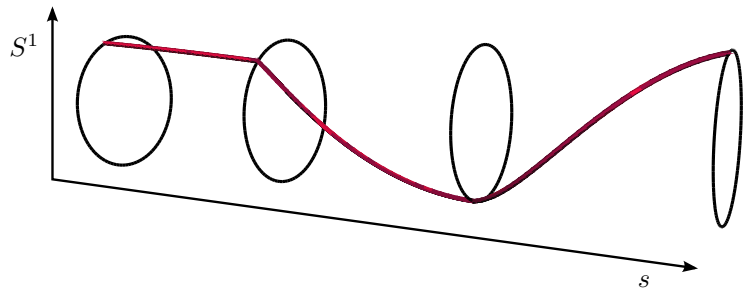

Figure 2: First-order geodesic finite element function on the unit circle S^1.

for a suitable p. From the coerciveness of W follows the coerciveness of j as a function of u and v. Impose the Dirichlet boundary conditions

$$\varphi(0) = (r_0, q_0) \qquad \text{and} \qquad \varphi(l) = (r_l, q_l). \tag{15}$$

The problem of finding stable equilibrium configurations of Cosserat rods can then be written as the optimization problem

$$\text{minimize } j \text{ in } W^{1,p}([0,l], \mathrm{SE}(3)) \text{ subject to (9) and (15).} \tag{16}$$

Existence and regularity of solutions to this problem have been shown by Seidman and Wolfe [15]. The main difficulty is the condition (9) on the preservation of orientation, since it is a strict inequality and hence the admissible set is open. Nevertheless, the following regularity result holds.

Theorem 3.1 (Seidman and Wolfe [15], Thm. 4.24)**.** *Let* $(\mathbf{u}(\varphi), \mathbf{v}(\varphi))$ *be a solution of the minimization problem* (14)*, subject to the orientation condition* (9) *and the boundary conditions* (15)*. Then* $(\mathbf{u}(\varphi), \mathbf{v}(\varphi))$ *is in* $(C^1[0,1])^6$ *and, with the forces* n *and moments* m *given by* (12)*, satisfies the strong equilibrium equations* (10), (11)*.*

Seidman and Wolfe also showed that solutions of nonlinear rod problems are generally not unique.

4 Geodesic Finite Elements

In this section we introduce geodesic finite element spaces as a generalization of first-order finite element spaces to problems involving functions with values in a nonlinear manifold. To our knowledge geodesic finite elements have not previously appeared in the literature. With the application to rod problems in mind we stick to one-dimensional domain spaces. However, an extension to higher dimensions may be useful for nonlinear shell models or micropolar materials and is the subject of a forthcoming paper. We first discuss geodesic finite elements for general Riemannian manifolds. Chapter 5 then specializes some of the results for SE(3), the configuration manifold of a Cosserat rod cross-section.

Definition Let M be a Riemannian manifold that is geodesically complete, and consider functions from an interval $[0, l]$ to M. Introduce a grid $\mathcal{G}$ on $[0, l]$ by subdividing the interval in finitely many subintervals $[l_i, l_{i+1}]$ of not necessarily the same size. Call n the number of grid vertices and $h = \max_i |l_{i+1} - l_i|$ the maximum element size. To motivate the definition of geodesic finite elements note that a standard first-order finite element function ϕ_h is a continuous function such that for all elements $[l_i, l_{i+1}]$ the function value $\phi_h(s)$ at $s \in [l_i, l_{i+1}]$ is given by linear interpolation between $\phi_h(l_i)$ and $\phi_h(l_{i+1})$. Geodesic finite element functions are obtained by replacing linear interpolation by interpolation along a geodesic.

Definition 4.1 (Geodesic finite elements)**.** *Let $\mathcal{G}$ be a grid on $[0, l]$ and M a Riemannian manifold that is geodesically complete. We call $\phi_h : [0, l] \to M$ a geodesic finite element function for M if it is continuous and, for each element $[l_i, l_{i+1}]$ of $\mathcal{G}$, $\phi_h|_{[l_i, l_{i+1}]}$ is a minimizing geodesic on M. The space of all such functions will be denoted by V_h^M.*

Example 1. Let S^1 be the unit sphere in $\mathbb{R}^2$ with a coordinate system given by the angle α. Then $V_h^{S^1}$ is the set of all continuous functions $\phi_h : [0, l] \to S^1$ such that the restriction of ϕ_h to an element $[l_i, l_{i+1}]$ is of the form

$$\phi_h|_{[l_i, l_{i+1}]}(s) = \alpha_i + m\left(\frac{s - l_i}{l_{i+1} - l_i}\right),$$

with $|m| \leq \pi$ (see Fig. 2).
Example 2. If $M = \mathbb{R}^m$ for $m \geq 1$ then V_h^M is precisely the standard m-valued first-order finite element space.

We will now explore a few properties of geodesic finite element spaces. Note first that V_h^M is a linear space if and only if M is. Therefore, unless M is a linear space, there is no such thing as a basis of V_h^M. In particular, there is no nodal basis. Also, we would like to point out that even though this article introduces geodesic finite elements in the context of the rotation group SO(3), the construction does not rely on a possible Lie-group structure of M.

Next we show that geodesic finite elements are conforming in the sense that $V_h^M \subset H^1([0, l], M) = W^{1,2}([0, l], M)$. The Sobolev space $W^{1,2}$ has been defined in (13). Since the condition that point values of functions from V_h^M be on M almost everywhere holds by definition, we are left to show that $V_h^M \subset H^1([0, l], \mathbb{R}^k)$ for some isometrical embedding $M \to \mathbb{R}^k$. For this we use the following simple theorem.

Theorem 4.1 (Braess [4], Thm. 5.2)**.** *A piecewise differentiable function $v : [0, l] \to \mathbb{R}$ is in $H^1([0, l], \mathbb{R})$ if and only if it is continuous.*

Hence geodesic finite element functions are in $H^1([0, l], \mathbb{R}^k)$ if they are differentiable on each element. This follows from the (local) characterization of geodesics as the images of straight lines under the exponential map (which is a diffeomorphism), and the smoothness of the embedding of M in $\mathbb{R}^k$.

Coefficient Vectors The linear finite element method is based on the natural isomorphism between finite element functions and coefficient vectors. Let V_h be a space of first-order finite element functions mapping into $\mathbb{R}^m$ for some $m \geq 1$,

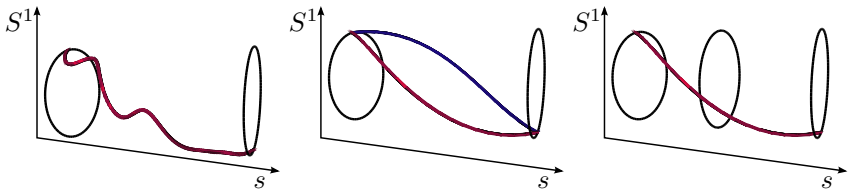

Figure 3: Left: a smooth function $\phi : [0, l] \to S^1$ with $\phi(0) = 0$ and $\phi(l) = \pi$. Center: nodal interpolation on a grid $\mathcal{G}$ consisting of a single element yields two minimizing geodesics. Right: if the grid is refined the nodal interpolation is unique.

and let v_h be a function in V_h. The coefficient vector $\bar{v} \in \mathbb{R}^{m\times n}$ corresponding to v_h is obtained by pointwise evaluation of v_h at the grid vertices. Let $C([0, l], \mathbb{R}^m)$ be the space of continuous functions mapping $[0, l]$ to $\mathbb{R}^m$. For a given grid $\mathcal{G}$ we denote the pointwise evaluation operator by

$$\mathcal{E} : C([0, l], \mathbb{R}^m) \to \mathbb{R}^{m\times n}, \qquad (\mathcal{E}(v_h))_i = v_h(l_i) \in \mathbb{R}^m,\ i = 0, \ldots, n-1.$$

Its inverse, the prolongation $\mathcal{E}^{-1}$ is set-valued and maps a coefficient vector $\bar{v}$ in $\mathbb{R}^{m\times n}$ to the set of all continuous functions that have $\bar{v}$ as their pointwise evaluation at the grid vertices. However, the prolongation $\mathcal{E}^{-1}\bar{v} \subset C([0, l], \mathbb{R}^m)$ contains only a single element in V_h for each $\bar{v} \in \mathbb{R}^{m\times n}$.

This may not be true if $\mathbb{R}^m$ is replaced with a general manifold M. There one would hope for an isomorphism between V_h^M and M^n, the n-fold product of M. However, while there is always a unique straight line segment between two points in a Euclidean space, there may be more than one minimizing geodesic between two given points on M. For example, if $M = S^1$ and $\bar{\phi}_0, \bar{\phi}_1 \in S^1$ differ by an angle of π, there are two minimizing geodesics from $\bar{\phi}_0$ to $\bar{\phi}_1$, namely one going in clockwise and one in counterclockwise direction (Fig. 3, center).

On certain manifolds it can be shown that minimizing geodesics are always unique. An example are the hyperbolic spaces H^d [8, Prop. 8.3.1], and of course the linear spaces. If minimizing geodesics are not unique, we can at least show a local property which is sufficient for practical applications. We need the following classical result [8, Thm. 3.3.7 and Rem. 3.3.8].

Lemma 4.1. *For each $p \in M$ there is a nonempty neighborhood U of p in M such that for all $q, \tilde{q} \in U$ there is a unique minimizing geodesic from q to $\tilde{q}$.*

Example 3. For two points $\alpha, \beta \in S^1$ the minimizing geodesic from α to β is unique if $\operatorname{dist}(\alpha, \beta) < \pi$.

The radius of the largest geodesic ball $B(p)$ at p with $B(p) \subset U$ is called the *injectivity radius* at p and denoted by $\operatorname{inj}(p)$. The infimum of the injectivity radii over all of M is called the injectivity radius of M and denoted by $\operatorname{inj}(M)$.

Let $\phi : [0, l] \to M$. We say that ϕ is Lipschitz continuous with Lipschitz constant L if

$$\operatorname{dist}(\phi(a), \phi(b)) \le L|a - b|$$

holds for all $a, b \in [0, l]$, where $\operatorname{dist}(\cdot, \cdot)$ is the geodesic distance on M. Using these preliminaries we can show that the possible nonuniqueness of geodesic interpolation can be disregarded if the grid is fine enough.

Lemma 4.2. *Let* $\operatorname{inj}(M) > 0$ *and* $\phi : [0, l] \to M$ *be Lipschitz continuous with Lipschitz constant* L*. Let* $\mathcal{G}$ *be a grid with maximum element size* $h < \operatorname{inj}(M)/L$*. Then, setting* $\bar{\phi} = \mathcal{E}(\phi) \in M^n$*, the inverse of* $\mathcal{E}$ *at* $\bar{\phi}$ *has only a single element in* V_h^M*. Furthermore, if* $h < \epsilon \operatorname{inj}(M)/L$ *for some* $\epsilon \in (0, 1)$*, the inverse of* $\mathcal{E}$ *has only a single element in* V_h^M *for each* $\tilde{\phi}$ *in a neighborhood of* $\bar{\phi}$*.*

Proof. We note first that by Lemma 4.1 a minimizing geodesic joining p and q is unique if $\operatorname{dist}(p, q) < \operatorname{inj}(M)$. If h is less than $\operatorname{inj}(M)/L$ and

$$\bar{\phi} = \mathcal{E}(\phi) \in M^n, \qquad \bar{\phi}_i = \phi(l_i), \qquad 0 \le i < n$$

we get

$$\operatorname{dist}(\bar{\phi}_i, \bar{\phi}_{i+1}) \le L|l_i - l_{i+1}| \le Lh \le \operatorname{inj}(M)$$

for all $0 \le i < n - 1$. Hence there is a unique minimizing geodesic from $\bar{\phi}_i$ to $\bar{\phi}_{i+1}$ and a unique prolongation of $\bar{\phi}$ into V_h^M.

Let now $\mathcal{G}$ be such that $h = \epsilon \operatorname{inj}(M)/L$ with $\epsilon \in (0, 1)$. Then $\operatorname{dist}(\bar{\phi}_i, \bar{\phi}_{i+1}) \le \epsilon \operatorname{inj}(M)$ for all $0 \le i < n - 1$. Define $\epsilon^* = \frac{(1-\epsilon)}{2} \operatorname{inj}(M)$ and set $B_{\epsilon^*}(\bar{\phi}_i)$ and $B_{\epsilon^*}(\bar{\phi}_{i+1})$ the geodesic balls of radius ϵ^* around $\bar{\phi}_i$ and $\bar{\phi}_{i+1}$ in M, respectively. Then for any $\tilde{\phi}_i \in B_{\epsilon^*}(\bar{\phi}_i)$ and $\tilde{\phi}_{i+1} \in B_{\epsilon^*}(\bar{\phi}_{i+1})$ we have, by the triangle inequality,

$$\operatorname{dist}(\tilde{\phi}_i, \tilde{\phi}_{i+1}) \le \operatorname{dist}(\tilde{\phi}_i, \bar{\phi}_i) + \epsilon \operatorname{inj}(M) + \operatorname{dist}(\bar{\phi}_{i+1}, \tilde{\phi}_{i+1}) \le \operatorname{inj}(M).$$

Hence if $B_{\epsilon^*}(\bar{\phi})$ is the geodesic ball in M^n of radius ϵ^* around $\bar{\phi} \in M^n$ there is a unique prolongation for all $\tilde{\phi} \in B_{\epsilon^*}(\bar{\phi})$ into V_h^M. □

This lemma implies that for a given problem with a Lipschitz-continuous solution we can always find a grid fine enough such that we can disregard the distinction between V_h^M and M^n in the vicinity of the solution. In this vicinity, V_h^M inherits the manifold structure of M^n, because short geodesics depend differentiably on their endpoints (Lemma 2.1). If M is a Lie group, V_h^M also locally inherits the Lie group properties of M^n. By a density argument, these results also extend to problems with solutions in H^1.

Interpolation Error Using the techniques from Lemma 4.2 we can also bound the interpolation error. For this define the Lagrange interpolation operator

$$I_h : C([0, l], M) \to V_h^M$$

by the condition

$$I_h \phi(l_i) = \phi(l_i), \qquad \forall\, l_i \in \mathcal{G},$$

assuming that the grid $\mathcal{G}$ is fine enough for I_h to be single-valued. Note that $I_h \phi = (\mathcal{E}^{-1} \mathcal{E} \phi) \cap V_h^M$.

Lemma 4.3. *Let* $\phi : [0, l] \to M$ *be Lipschitz continuous. Then*

$$\max_{s \in [0,l]} \operatorname{dist}\big(\phi(s), I_h \phi(s)\big) \le 2hL,$$

where L *denotes the Lipschitz constant of* ϕ*.*

Proof. Let $s \in [l_i, l_{i+1}]$ be fixed for some $[l_i, l_{i+1}] \in \mathcal{G}$. Then

$$\begin{aligned} \operatorname{dist}\big(\phi(s), I_h\phi(s)\big) &\leq \operatorname{dist}\big(\phi(s), \phi(l_i)\big) + \operatorname{dist}\big(\phi(l_i), I_h\phi(s)\big) \\ &\leq L(s-l_i) + \frac{s-l_i}{l_{i+1}-l_i} \operatorname{dist}\big(\phi(l_i), \phi(l_{i+1})\big) \\ &\leq L(s-l_i) + L(s-l_i) \\ &\leq 2Lh. \end{aligned}$$

Since this holds for all $s \in [l_i, l_{i+1}]$ and all elements $[l_i, l_{i+1}]$, $0 \leq i < n+1$, we have

$$\max_{0\leq i<n-1} \max_{s\in[l_i,l_{i+1}]} \operatorname{dist}\big(\phi(s), I_h\phi(s)\big) \leq 2Lh,$$

which was asserted. □

Objectivity The interpolation along geodesics has an invariance property that is very desirable in the context of mechanics. Recall that an energy functional $J : W^{1,p}([0,l], M) \to \mathbb{R}$ is called *objective* or *frame-invariant*, if

$$J(Q\phi(x)) = J(\phi(x)) \qquad \forall s \in [0,l]$$

for all $Q \in \mathrm{SO}(3)$, where $Q\phi$ is an isometric left action of $\mathrm{SO}(3)$ on M. An objective functional on a function space leads to an objective *algebraic* functional $\bar{J} : M^n \to \mathbb{R}$ only if the prolongation $\mathcal{E}^{-1} : M^n \to V_h^M \subset H^1([0,l], M)$ is invariant under the same action of $\mathrm{SO}(3)$. For geodesic finite elements, this is indeed the case.

Lemma 4.4 (Objectivity)**.** *Let $\bar{v} \in M^n$ be a coefficient vector and $\mathcal{E}^{-1}\bar{v} \in V_h^M$ the corresponding geodesic finite element function, which we assume to be unique. Let G be a Lie group that acts isometrically on M. Then*

$$Q(\mathcal{E}^{-1}\bar{v}) = \mathcal{E}^{-1}(Q\bar{v})$$

for all $Q \in G$.

Proof. It is sufficient to consider a single element $[l_i, l_{i+1}]$ of $\mathcal{G}$ and to show that $\gamma[Qv_i, Qv_{i+1}](s) = Q\gamma[v_i, v_{i+1}](s)$ for all $Q \in G$, $s \in [0,1]$, where $\gamma[v_i, v_{i+1}](\cdot)$ denotes the geodesic interpolation from v_i to v_{i+1}. We only use the metric properties of M. If M is a Lie group, the assertion can be shown directly using the formula (7).

We first show that

$$\operatorname{dist}(Qv_i, Q\gamma[v_i, v_{i+1}](s)) = \operatorname{dist}(Qv_i, \gamma[Qv_i, Qv_{i+1}](s)). \tag{17}$$

To see this note first that $\operatorname{dist}(v_i, \gamma[v_i, v_{i+1}](s)) = \operatorname{dist}(Qv_i, Q\gamma[v_i, v_{i+1}](s))$, because Q acts isometrically. On the other hand, by the definition of the geodesic interpolation we have

$$s = \frac{\operatorname{dist}(v_i, \gamma[v_i, v_{i+1}](s))}{\operatorname{dist}(v_i, v_{i+1})} = \frac{\operatorname{dist}(Qv_i, \gamma[Qv_i, Qv_{i+1}](s))}{\operatorname{dist}(Qv_i, Qv_{i+1})}.$$

Again using the isometry property of Q, the denominators of this must be equal, and hence also the numerators. Thus (17) follows. Similarly, we can show that

$$\operatorname{dist}(Qv_{i+1}, Q\gamma[v_i, v_{i+1}](s)) = \operatorname{dist}(Qv_{i+1}, \gamma[Qv_i, Qv_{i+1}](s)).$$

Together, it follows that $Q\gamma[v_i, v_{i+1}](s)$ must be on the unique minimizing geodesic from Qv_i to Qv_{i+1}, because if it wasn't, there would be a second path from Qv_i to Qv_{i+1} (via $Q\gamma[v_i, v_{i+1}](s)$) realizing the geodesic distance. This proves the lemma, because with both $Q\gamma[v_i, v_{i+1}](s)$ and $\gamma[Qv_i, Qv_{i+1}](s)$ on the unique minimizing geodesic from Qv_i to Qv_{i+1} and (17), the two points $Q\gamma[v_i, v_{i+1}](s)$ and $\gamma[Qv_i, Qv_{i+1}](s)$ must be equal. □

Implementation of Geodesic Finite Elements For the actual implementation of a finite element assembler explicit interpolation formulas are needed. Assume that the energy functional depends only on function values and first derivatives, i.e.,

$$J(\phi) = \int_{[0,l]} W(\phi(s), \phi'(s))\, ds, \qquad \phi \in W^{1,p}([0,l], M),$$

and let $\mathcal{G}$ be a grid on $[0, l]$. Then, just as in the Euclidean finite element method, J (and its gradient and the Hesse matrix) can be computed as sums of element-wise contributions. For each element $[l_i, l_{i+1}]$ consider the affine mapping F from the reference element $[0, 1]$ to $[l_i, l_{i+1}]$. Let $\gamma[p, q](\cdot) : [0, 1] \to M$ be the geodesic from p to q in M and $\gamma'[p, q](\cdot) : [0, 1] \to TM$ its derivative. Then, for a geodesic finite element function $\phi_h \in V_h^M$ with coefficients v_i, $0 \le i < n$,

$$\begin{aligned}\int_{[l_i,l_{i+1}]} & W(\phi_h(s), \phi_h'(s))\, ds \\ &= \int_{[0,1]} W\big(\gamma[v_i, v_{i+1}](s), \nabla(F^{-1})^T \gamma'[v_i, v_{i+1}](s)\big) |\det F|\, ds,\end{aligned}$$

and the integral on the right can be computed using numerical quadrature. The expressions for γ and γ' are the only information needed to implement geodesic finite elements for a given manifold M. Concrete formulas for $M = \mathrm{SO}(3)$ using quaternion coordinates will be given in the following chapter.

5 Geodesic Finite Elements on SE(3)

In this chapter we work out geodesic finite elements for Cosserat rod problems. Remember that configurations of Cosserat rods are described by functions mapping intervals onto the special Euclidean group $\mathrm{SE}(3) = \mathbb{R}^3 \rtimes \mathrm{SO}(3)$. Using the results about products of spaces we know that this is a Riemannian manifold with tangent spaces

$$T_{(r,q)}\mathrm{SE}(3) = T_r\mathbb{R}^3 \oplus T_q\mathrm{SO}(3). \tag{18}$$

The metric is given by

$$\begin{aligned} g_{(r,q)}(\cdot,\cdot) &: T_{(r,q)}\mathrm{SE}(3) \times T_{(r,q)}\mathrm{SE}(3) \to \mathbb{R} \\ g_{(r,q)}\big((w_1, q\hat{v}_1), (w_2, q\hat{v}_2)\big) &= \langle w_1, w_2\rangle + \langle v_1, v_2\rangle \end{aligned} \tag{19}$$

and the exponential map is

$$\begin{aligned} \exp_{(r,q)} &: T_{(r,q)}\mathrm{SE}(3) \to \mathrm{SE}(3) \\ \exp_{(r,q)}(w, q\hat{v}) &= (r + w, q \exp \hat{v}). \end{aligned} \tag{20}$$

The following result is a direct consequence of Lemma 2.2 and the completeness of Euclidean spaces.

Lemma 5.1. *SE*(3) *is geodesically complete.*

The injectivity radius of SE(3) can be computed exactly. As minimizing geodesics in $\mathbb{R}^3$ are always unique we have $\operatorname{inj}(\mathrm{SE}(3)) = \operatorname{inj}(\mathrm{SO}(3))$. The injectivity radius of the special orthogonal group SO(3) is given by the following well-known lemma, proved, e.g., in [13].

Lemma 5.2. *Let* $p, q \in SO(3)$. *Then* $\operatorname{dist}(p, q) \leq \pi$. *If* $\operatorname{dist}(p, q) < \pi$ *then there is a unique minimizing geodesic from* p *to* q. *If* $\operatorname{dist}(p, q) = \pi$ *then there are precisely two minimizing geodesics from* p *to* q.

Hence, to a given coefficient vector $\bar{v} \in \mathrm{SE}(3)^n$ and a grid $\mathcal{G}$, there corresponds a unique finite element function if $\operatorname{dist}(v_i, v_{i+1}) < \pi$ for all $0 \leq i < n-1$ (this condition is not necessary, though).

Interpolation Formulas The continuous rod energy functional j defined in (14) depends only on function values and first derivatives of the configuration φ. As shown in the previous chapter, all that is needed to implement the evaluation of j are the formulas for geodesics $\gamma_{\mathrm{SE}(3)}[p, q](\cdot) : [0, 1] \to \mathrm{SE}(3)$ and their derivatives $\gamma'_{\mathrm{SE}(3)}[p, q](\cdot) : [0, 1] \to T\mathrm{SE}(3)$. These will be derived now.

By (20), the expression for geodesics on the product manifold SE(3) factors in an expression for geodesics on $\mathbb{R}^3$ and an expression for geodesics on SO(3). Since geodesics in $\mathbb{R}^3$ are simply straight lines we focus on the second factor SO(3). Using quaternion coordinates and the formulas (8) for the exponential map on SO(3), explicit expressions can be derived for

$$\gamma_{\mathrm{SO}(3)}[p, q](\cdot) : [0, 1] \to \mathrm{SO}(3).$$

In the following we drop the subscript for simplicity.

For any geodesic on SO(3) that connects p to q there is a tangent vector $p\hat{v} \in T_p\mathrm{SO}(3)$ such that $\exp_p p\hat{v} = q$. Since $\exp_p$ is a local diffeomorphism (hence locally invertible) we can write $\hat{v} = \exp^{-1}(p^{-1}q)$, where we have also used (7). We use (8) and the hat map (6) to obtain that the geodesic distance between p and q is $|\hat{v}| = |v| = 2\arccos((p^{-1}q)_4)$ and that

$$v_j = \frac{(p^{-1}q)_j |v|}{\sin \frac{|v|}{2}}, \qquad j = 1, 2, 3. \tag{21}$$

The interpolation between p and q along the connecting geodesic induced by $\hat{v}$ is then

$$\gamma[p, q](s) = \exp_p sp\hat{v} = p \exp s\hat{v}, \tag{22}$$

with $\hat{v}$ given by (21) and the hat map. Note that the symmetry property $\gamma[p, q](s) = \gamma[q, p](1 - s)$ can be shown by direct calculation. Formula (22) corresponds to (4.7) in the article of Crisfield and Jelenić [6].

Next we compute the tangent vector of a geodesic from p to q at $s \in [0, 1]$. By (22) and the chain rule we get

$$\gamma'[p, q](s) = \left.\frac{\partial \gamma[p, q](\cdot)}{\partial s}\right|_s = p \left.\frac{\partial \exp}{\partial v}\right|_{s\hat{v}} \cdot \hat{v}.$$

Using quaternion coordinates on SO(3) and identifying $\mathfrak{so}(3)$ with $\mathbb{R}^3$, the derivative $\frac{\partial \exp}{\partial v}$ is a 4×3 matrix. The explicit formula can be found in [13, App. A].

Minimization Formulations We now write down the discrete version of the rod minimization problem (16). Let $\mathcal{G}$ be a grid on $[0, l]$ with n vertices and maximum element size h. Let $\varphi_0, \varphi_l \in \mathrm{SE}(3)$ be given Dirichlet boundary data. We want to

$$\text{minimize } j \text{ in } V_h^{\mathrm{SE}(3)} \tag{23}$$

subject to

$$\varphi_h(0) = \varphi_0, \qquad \varphi_h(l) = \varphi_l,$$

and the nonpenetration condition (9), where

$$j(\varphi) = \int_{[0,l]} W(\mathsf{u}(\varphi) - \hat{\mathsf{u}}, \mathsf{v}(\varphi) - \hat{\mathsf{v}})\, ds$$

is the hyperelastic energy functional (14).

Using the prolongation operator $\mathcal{E}^{-1} : \mathrm{SE}(3)^n \to V_h^{\mathrm{SE}(3)}$ we can also write down an algebraic formulation of the same problem. Let h be sufficiently small for $\mathcal{E}^{-1}$ to be single-valued. Then the algebraic problem is to

$$\text{minimize } \bar{\jmath} \text{ in } \mathrm{SE}(3)^n$$

with the algebraic rod energy functional

$$\bar{\jmath}(\bar{\varphi}) = \int_{[0,l]} W\big(\mathsf{u}(\mathcal{E}^{-1}(\bar{\varphi})) - \hat{\mathsf{u}}, \mathsf{v}(\mathcal{E}^{-1}(\bar{\varphi})) - \hat{\mathsf{v}}\big)\, ds, \tag{24}$$

subject to (9) and the boundary conditions

$$\bar{\varphi}_0 = \varphi_0 \qquad \text{and} \qquad \bar{\varphi}_{n-1} = \varphi_l.$$

Using Lemma 2.1 and the fact that $\mathbf{u}$, $\mathbf{v}$, and W are all differentiable functions we can show the following.

Lemma 5.3. *The algebraic rod functional $\bar{\jmath} : SE(3)^n \to \mathbb{R}$ depends differentiably on its arguments.*

6 A Riemannian Trust-Region Solver for Cosserat Rod Problems

We have seen that algebraic geodesic finite element problems have the form

$$\text{minimize } \bar{\jmath} \text{ in } M,$$

where M is a product manifold and $\bar{\jmath}$ a functional that maps (a subset of) M to $\mathbb{R}$. For such minimization problems Absil et al. [1] introduced a Riemannian trust-region method. In this section we show how this method can be used to solve Cosserat rod problems that have been discretized by geodesic finite elements. From the underlying Newton idea trust-region solvers inherit local

superlinear convergence; however, they are also globally convergent. While Newton-type methods for Cosserat rods seem to be standard [14, 16], to our knowledge no trust-region algorithm for Cosserat rods has been published.

There are two obstacles to generalizing standard trust-region methods to nonlinear spaces. First, the concept of a local quadratic model of the objective function has to be revised. Also, as there is no canonical addition defined on a manifold, the update procedure $x_{\nu+1} = x_\nu + v_\nu$ needs to be replaced by something more general. We will now briefly present the generalization of the trust-region algorithm to Riemannian manifolds as introduced by Absil et al. [1] and show how the general algorithm specializes when the underlying space is the set $\mathrm{SE}(3)^n$ of configurations of an algebraic Cosserat rod problem.

Riemannian Trust-Region Methods Let M be a Riemannian manifold with metric g. The basic idea of the Riemannian trust-region algorithm is that in a neighborhood of a point $q \in M$ the objective function can be lifted onto the tangent space T_qM. There, a vector space trust-region subproblem can be solved and the result transported back onto M. In the case of $M = \mathrm{SE}(3)^n$, the exponential map can be used for the transport, since an explicit formula for its evaluation is available. More formally, let $q_\nu \in M$, $\nu \in \mathbb{N}$ be the current iterate. Using $\exp_{q_\nu}$ to lift the objective function j onto the tangent space $T_{q_\nu}M$ we obtain the lifted functional

$$\begin{aligned} \hat{\jmath}_\nu &: T_{q_\nu}M \to \mathbb{R} \\ \hat{\jmath}_\nu(v) &= j(\exp_{q_\nu} v). \end{aligned}$$

Let $\rho_\nu \in \mathbb{R}$ be the current trust-region radius. The Riemannian structure g turns $T_{q_\nu}M$ into a Banach space with the norm $\|\cdot\|_{g_{q_\nu}} = \sqrt{g_{q_\nu}(\cdot,\cdot)}$. There, the trust-region subproblem reads

$$v_\nu = \arg \min_{\substack{v \in T_{q_\nu}M \\ \|v\|_{g_{q_\nu}} \le \rho_\nu}} m_\nu(v) \tag{25}$$

with the quadratic, but not necessarily convex model

$$m_\nu(v) = \hat{\jmath}_\nu(0) + g_{q_\nu}(\nabla \hat{\jmath}_\nu(0), v) + \frac{1}{2} g_{q_\nu}(\nabla^2 \hat{\jmath}_\nu(0) v, v). \tag{26}$$

Here $\nabla \hat{\jmath}_\nu(0)$ is the gradient and and $\nabla^2 \hat{\jmath}_\nu(0)$ the Hessian of $\hat{\jmath}$, both evaluated at $0 \in T_{q_\nu}M$. Note that the problem is independent of a specific coordinate system on $T_{q_\nu}M$. As a minimization problem of a continuous function on a compact set, (25) has at least one solution. A solution $v_\nu \in T_{q_\nu}M$ of (25) generates the new iterate by

$$q_{\nu+1} = \exp_{q_\nu} v_\nu.$$

As for trust-region methods in linear spaces, the quality of a correction step v_ν is estimated by comparing the functional decrease and the model decrease. If the quotient

$$\kappa_\nu = \frac{j(q_\nu) - j(\exp_{q_\nu} v_\nu)}{m_\nu(0) - m_\nu(v_\nu)}$$

is smaller than a fixed value η_1, then the step is rejected, and v_ν is recomputed for a smaller trust-region radius ρ. If not, the step is accepted. If κ_ν is larger

than a second value η_2, the trust-region radius is enlarged for the next step. Common values are $\eta_1 = 0.01$ and $\eta_2 = 0.9$ [5].

For this method, Absil et al. [1] proved global convergence to first-order stationary points, and, depending on the exactness of the inner solver, locally superlinear or even locally quadratic convergence.

Application to Cosserat Rod Problems When applying the general Riemannian trust-region algorithm to the discrete Cosserat rod problem (23), the manifold M is $\mathrm{SE}(3)^n$, with n the number of grid vertices. For simplicity we will ignore the orientation-preserving inequality (9). We denote elements of $\mathrm{SE}(3)^n$ by

$$(r, q) = \prod_{i=0}^{n-1} (r_i, q_i), \qquad r_i \in \mathbb{R}^3,\ q_i \in \mathrm{SO}(3).$$

At any $(r, q) \in \mathrm{SE}(3)^n$, by (18) and Lemma 2.3 the tangent space is

$$T_{(r,q)}\mathrm{SE}(3)^n = \bigoplus_{i=0}^{n-1} \big(T_{r_i}\mathbb{R}^3 \oplus T_{q_i}\mathrm{SO}(3)\big) = \bigoplus_{i=0}^{n-1} \big(\mathbb{R}^3 \oplus q_i\mathbb{A}^3\big),$$

where the spaces $q_i\mathbb{A}^3$ have been defined in (5). The exponential map $\exp_{(r,q)} : T_{(r,q)}\mathrm{SE}(3)^n \to \mathrm{SE}(3)^n$ can be written as

$$\exp_{(r,q)}(w, q\hat{v}) = \prod_{i=0}^{n-1} \big(r_i + w_i,\ q_i \exp \hat{v}_i\big), \tag{27}$$

where we have used (4) together with (7).

The functional to be considered is the algebraic Cosserat rod energy $\bar{\jmath}$ defined in (24) and repeated here for convenience:

$$\begin{aligned} \bar{\jmath} \quad &: \quad \mathrm{SE}(3)^n \to \mathbb{R} \\ \bar{\jmath}(\bar{\varphi}) \quad &= \quad \int_{[0,l]} W\big(\mathsf{u}(\mathcal{E}^{-1}(\bar{\varphi})) - \hat{\mathsf{u}}, \mathsf{v}(\mathcal{E}^{-1}(\bar{\varphi})) - \hat{\mathsf{v}}\big)\, ds. \end{aligned} \tag{28}$$

The prolongation mapping $\mathcal{E}^{-1} : \mathrm{SE}(3)^n \to V_h^{\mathrm{SE}(3)}$ is given element-wise. Let $[l_i, l_{i+1}]$ be an element of $\mathcal{G}$ and let $s \in [l_i, l_{i+1}]$, then

$$\begin{aligned} \mathcal{E}^{-1}(\bar{\varphi})(s) \quad &= \quad \gamma_{\mathrm{SE}(3)}[\bar{\varphi}_i, \bar{\varphi}_{i+1}](F_i^{-1}(s)) \\ &= \quad \big(\gamma_{\mathbb{R}^3}[r_i, r_{i+1}](F_i^{-1}(s)),\ \gamma_{\mathrm{SO}(3)}[q_i, q_{i+1}](F_i^{-1}(s))\big), \end{aligned} \tag{29}$$

where $\bar{\varphi}_i = (r_i, q_i)$ and F_i is the affine mapping from the reference element $[0, 1]$ to $[l_i, l_{i+1}]$. Since $\mathbb{R}^3$ is linear the geodesics there are line segments and geodesic finite elements degenerate to standard finite elements. Using the vector-valued nodal basis functions $\boldsymbol{\psi}_k^j : [0, l] \to \mathbb{R}^3$ and the fact that $F_i(s) = l_i + s(l_{i+1} - l_i)$ we can rewrite (29) as

$$\mathcal{E}^{-1}(\bar{\varphi})(s) = \left(\sum_{\substack{j \in \{0,1,2\} \\ k \in \{i, i+1\}}} r_k^j \boldsymbol{\psi}_k^j(s),\ \gamma_{\mathrm{SO}(3)}[q_i, q_{i+1}]\Big(\frac{s - l_i}{l_{i+1} - l_i}\Big) \right).$$

Remark 6.1. Note that the Riemannian trust-region method is a descent method, and therefore the sequence of iterates remains within the sublevel set of the first iterate. Since $\bar{\jmath}$ is assumed to be coercive, these sublevel sets are bounded. By Lemma 4.2 we know that if the grid is fine enough there is a neighborhood $U \subset \mathrm{SE}(3)^n$ of the discrete solution such that there is a one-to-one correspondence between geodesic finite element functions in $V_h^{\mathrm{SE}(3)}$ and coefficient vectors in U. Hence for initial iterates close enough to the solution we can disregard the distinction between $V_h^{\mathrm{SE}(3)}$ and $\mathrm{SE}(3)^n$.

We now lift $\bar{\jmath}$ onto the tangent bundle of $\mathrm{SE}(3)^n$. Let $\nu \in \mathbb{N}$ be the iteration number and $(r_\nu, q_\nu) \in \mathrm{SE}(3)^n$ the current iterate of a Riemannian trust-region method. Then, using the exponential map (27), the lifted algebraic rod functional at (r_ν, q_ν) is

$$\begin{aligned} \hat{\jmath}_\nu &: T_{(r_\nu,q_\nu)}\mathrm{SE}(3)^n \to \mathbb{R} \\ \hat{\jmath}_\nu(w, q_\nu\hat{v}) &= \bar{\jmath}(\exp_{(r_\nu,q_\nu)}(w, q_\nu\hat{v})) = \bar{\jmath}(r_\nu + w, q_\nu \exp\hat{v}). \end{aligned} \tag{30}$$

In order to obtain the quadratic model m_ν defined in (26), we need to compute the gradient $\nabla\hat{\jmath}_\nu$ and the Hesse matrix $\nabla^2\hat{\jmath}_\nu$ of the lifted functional $\hat{\jmath}_\nu$ at $0 \in T_{(r_\nu,q_\nu)}\mathrm{SE}(3)^n$. Using (19) we get

$$g_\nu(\nabla\hat{\jmath}_\nu, (w, q_\nu\hat{v})) = \langle \nabla_w\hat{\jmath}_\nu, w\rangle + \langle \nabla_v\hat{\jmath}_\nu, v\rangle$$

for all $(w, q_\nu\hat{v}) \in T_{(r_\nu,q_\nu)}\mathrm{SE}(3)^n$, where $\nabla_w, \nabla_v \in (\mathbb{R}^3)^n$ denote the gradients with respect to w and v, respectively. Using the canonical basis of $\mathbb{R}^3$, the coefficients of these gradients are the partial derivatives in the coordinate directions. To compute them, we first introduce the *algebraic strain measures*

$$\begin{aligned} \bar{\mathsf{u}}, \bar{\mathsf{v}} : \mathrm{SE}(3)^n &\to C([0,l], \mathbb{R}^3) \\ \bar{\mathsf{u}}(r,q) = \mathsf{u}(\mathcal{E}^{-1}(r,q)), &\qquad \bar{\mathsf{v}}(r,q) = \mathsf{v}(\mathcal{E}^{-1}(r,q)). \end{aligned}$$

They associate continuous strain functions to coefficient vectors in SE(3). Using (28) and (30) we get

$$\nabla_w\hat{\jmath}_\nu = \int_{[0,l]} \nabla_w W\big(\bar{\mathsf{u}}(\exp_{(r_\nu,q_\nu)}(w, q_\nu\hat{v})) - \hat{\mathsf{u}},\ \bar{\mathsf{v}}(\exp_{(r_\nu,q_\nu)}(w, q_\nu\hat{v})) - \hat{\mathsf{v}}\big)\, ds,$$

and likewise for $\nabla_v\hat{\jmath}$. Hence computing the gradient of the lifted energy functional $\hat{\jmath}_\nu$ amounts to computing the gradient of the lifted energy density

$$\widehat{W}_\nu(w, v) = W\big(\bar{\mathsf{u}}(\exp_{(r_\nu,q_\nu)}(w, q_\nu\hat{v})) - \hat{\mathsf{u}},\ \bar{\mathsf{v}}(\exp_{(r_\nu,q_\nu)}(w, q_\nu\hat{v})) - \hat{\mathsf{v}}\big).$$

Before continuing further we choose a specific energy density W. The simplest choice for a rod material is the linear elastic one. In this case, the energy is a quadratic function of the strains

$$W(\mathsf{w}, \mathsf{z}) = \frac{1}{2}\begin{pmatrix}\mathsf{w}\\ \mathsf{z}\end{pmatrix}^T \mathbf{W} \begin{pmatrix}\mathsf{w}\\ \mathsf{z}\end{pmatrix},$$

where $\mathbf{W} \in \mathbb{R}^{6\times 6}$ is symmetric and positive definite. A further simplification takes the matrix $\mathbf{W}$ to be diagonal, such that the energy density W takes the form

$$W(\mathsf{u} - \hat{\mathsf{u}}, \mathsf{v} - \hat{\mathsf{v}}) = \frac{1}{2}\sum_{i=1}^{3} K_i(\mathsf{u}_i - \hat{\mathsf{u}}_i)^2 + \frac{1}{2}\sum_{i=1}^{3} A_i(\mathsf{v}_i - \hat{\mathsf{v}}_i)^2, \tag{31}$$

with scalar parameters K_i, A_i, $i \in \{1,2,3\}$. Despite its simplicity, this material law is widely used [9, 16].

Let w_i^j, v_i^j be the coefficients of w, v pertaining to the i-th grid vertex and the canonical coordinate direction j. Then, for any $s \in [0,l]$, the coefficients of $\nabla_w \widehat{W}(s)$ and $\nabla_v \widehat{W}(s)$ at $0 \in T_{(r_\nu,q_\nu)}\mathrm{SE}(3)^n$ are given by

$$\frac{\partial \widehat{W}}{\partial w_i^j} = \sum_{m=1}^{3} A_m\big(\bar{\mathsf{v}}_m(r_\nu,q_\nu) - \hat{\mathsf{v}}_m\big)\frac{\partial}{\partial w_i^j}\bar{\mathsf{v}}_m(r_\nu + w, q_\nu \exp\hat{v}) \tag{32}$$

$$\begin{aligned}\frac{\partial \widehat{W}}{\partial v_i^j} &= \sum_{m=1}^{3} K_m\big(\bar{\mathsf{u}}_m(q_\nu) - \hat{\mathsf{u}}_m\big)\frac{\partial}{\partial v_i^j}\bar{\mathsf{u}}_m(q_\nu \exp\hat{v}) \\ &\quad + \sum_{m=1}^{3} A_m\big(\bar{\mathsf{v}}_m(r_\nu,q_\nu) - \hat{\mathsf{v}}_m\big)\frac{\partial}{\partial v_i^j}\bar{\mathsf{v}}_m(r_\nu + w, q_\nu \exp\hat{v}),\end{aligned} \tag{33}$$

where we have used that u does not depend on r. To compute the derivatives of the algebraic strains consider an element $[l_i, l_{i+1}]$ and $s \in [l_i, l_{i+1}]$. Then, for $j,m \in \{1,2,3\}$ and $k \in \{i, i+1\}$, the derivative of $\bar{\mathsf{v}}$ with respect to the finite element coefficients is

$$\frac{\partial}{\partial w_k^j}\bar{\mathsf{v}}_m(r_\nu + w, q_\nu \exp\hat{v})(s) = \Big\langle \frac{\partial \boldsymbol{\psi}_k^j}{\partial s}(s),\, \mathbf{d}_m\big(\gamma_{\mathrm{SO}(3)}[q_i, q_{i+1}](F_i^{-1}(s))\big)\Big\rangle$$

and

$$\begin{aligned}&\frac{\partial}{\partial v_k^j}\bar{\mathsf{v}}_m(r_\nu + w, q_\nu \exp\hat{v})(s) \\ &\qquad = \Big\langle r'(s),\, \frac{\partial \mathbf{d}_m}{\partial q}\cdot\frac{\partial}{\partial v_k^j}\gamma_{\mathrm{SO}(3)}[q_i \exp\hat{v}_i, q_{i+1}\exp\hat{v}_{i+1}](F_i^{-1}(s))\Big\rangle.\end{aligned}$$

The brackets denote the scalar product in $\mathbb{R}^3$. The derivatives of the rotational strain $\bar{\mathsf{u}}$ are, again for $j,m \in \{1,2,3\}$ and $k \in \{i, i+1\}$,

$$\begin{aligned}\frac{\partial}{\partial v_k^j}\bar{\mathsf{u}}_m(q_\nu \exp\hat{v})(s) &= 2\Big\langle \mathbf{B}_m\Big(\frac{\partial}{\partial v_k^j}\gamma_{\mathrm{SO}(3)}[q_i\exp\hat{v}_i, q_{i+1}\exp\hat{v}_{i+1}](F_i^{-1}(s))\Big), \\ &\qquad\qquad \gamma'_{\mathrm{SO}(3)}[q_i, q_{i+1}](F_i^{-1}(s))\Big\rangle \\ &\quad + 2\Big\langle \mathbf{B}_m\big(\gamma_{\mathrm{SO}(3)}[q_i, q_{i+1}](F_i^{-1}(s))\big), \\ &\qquad\qquad \frac{\partial}{\partial v_k^j}\gamma'_{\mathrm{SO}(3)}[q_i\exp\hat{v}_i, q_{i+1}\exp\hat{v}_{i+1}](F_i^{-1}(s))\Big\rangle.\end{aligned}$$

Unlike above, the brackets in this expression denote the scalar product in $\mathbb{R}^4$. Also recall that primes denote derivation with respect to s. As $\bar{\mathsf{u}}$ is independent of the centerline the derivatives $\partial\bar{\mathsf{u}}/\partial w_j^k$ are zero. The appendix of [13] shows how the preceding formulas are obtained.

Deriving (32) and (33) once more we get the coefficients of the Hessian matrix in a straightforward manner. Note that since $\hat{\jmath}_\nu$ is a functional on a linear space, its Hessian is symmetric. It involves second derivatives of the strain measures which, in principle, can also be computed analytically. However, the formulas

get fairly unwieldy. Fortunately, approximations to the Hessian matrix are allowed by the convergence theory of Riemannian trust-region methods. The examples in Chapter 7 use a finite-difference approximation to compute $\nabla^2 \hat{\jmath}$.

The standard Riemannian trust-region algorithm uses the Riemannian norm $\|\cdot\|_{g_{q_\nu}}$ to define the trust-region. In the finite-element context it is preferable to use a discretization of the L^2-norm. Let ψ_i be the scalar nodal basis function corresponding to vertex i and let

$$M_3 \in \mathbb{R}^{3n\times 3n}, \qquad (M_3)_{ij} = \mathrm{Id}_{3\times 3} \int_{[0,l]} \psi_i \psi_j \, ds$$

be the 3-valued mass matrix for the grid $\mathcal{G}$. Introduce the scaled L^2-norm

$$\begin{aligned} \|\cdot\|_{\alpha,(r,q)} &: T_{(r,q)}\mathrm{SE}(3)^n \to \mathbb{R} \\ \|(w,q\hat{v})\|^2_{\alpha,(r,q)} &= \alpha\langle w, M_3 w\rangle + \langle v, M_3 v\rangle, \end{aligned}$$

with a fixed scaling parameter $\alpha > 0$. This parameter is used to compensate for the possible scale differences between translational and rotational corrections. Alternatively, it is possible to use a generalization of the maximum norm on the tangent bundle of $\mathrm{SE}(3)^n$ by defining

$$\begin{aligned} \|\cdot\|_{\infty,\alpha,(r,q)} &: T_{(r,q)}\mathrm{SE}(3)^n \to \mathbb{R} \\ \|(w,q\hat{v})\|_{\infty,\alpha,(r,q)} &= \max\{\alpha\|w\|_\infty, \|v\|_\infty\}. \end{aligned} \tag{34}$$

For this norm, no matrix needs to be assembled and the trust region

$$\begin{aligned} K^{\mathrm{tr}}_{\infty,\nu} &= \big\{(w, q_\nu\hat{v}) \in T_{(r_\nu,q_\nu)}\mathrm{SE}(3)^n \;\big|\; \|(w,q_\nu\hat{v})\|_{\infty,\alpha,(r,q)} \le \rho_\nu\big\} \\ &\simeq [-\rho_\nu, \rho_\nu]^{6n} \end{aligned}$$

has a tensor-product structure.

In summary, we obtain the inner trust-region problem

$$(w_\nu, q_\nu\hat{v}_\nu) = \arg\min m_\nu(w, q_\nu\hat{v}), \tag{35}$$

where the minimization is over all $(w, q_\nu\hat{v}) \in T_{(r_\nu,q_\nu)}\mathrm{SE}(3)^n$ with

$$\|(w,q_\nu\hat{v})\|_{(r_\nu,q_\nu)} \le \rho_\nu,$$

using one of the norms introduced above and

$$m_\nu(w,q_\nu\hat{v}) = \hat{\jmath}_\nu(0) + g_\nu\big(\nabla\hat{\jmath}_\nu(0),(w,q_\nu\hat{v})\big) + \frac{1}{2}g_\nu\big(\nabla^2\hat{\jmath}_\nu(0)(w,q_\nu\hat{v}),(w,q_\nu\hat{v})\big).$$

With $(w_\nu, q_\nu\hat{v}_\nu)$ the solution of (35), the next iterate is given by

$$(r_{\nu+1}, q_{\nu+1}) = \exp_{(r_\nu,q_\nu)}(w_\nu, q_\nu\hat{v}_\nu) = (r_\nu + w_\nu, q_\nu \exp\hat{v}_\nu).$$

7 Numerical Results

We close this article by giving two short examples demonstrating the efficiency of the trust-region solver and estimating the convergence of the geodesic finite element discretization.

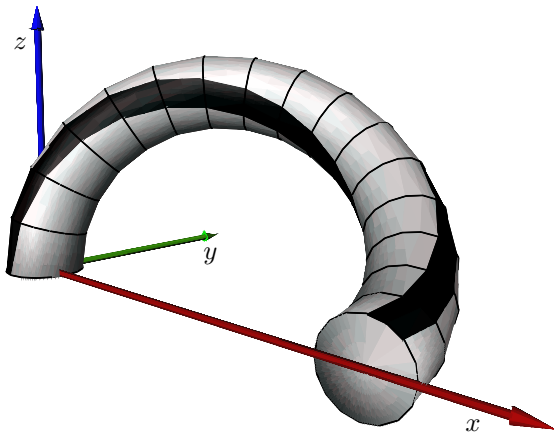

Figure 4: Solution of the example rod problem using a grid with 16 elements.

Consider a rod of unit length which, in its unstressed state, is completely straight and aligned with the z-axis. The rod is clamped at the origin, and the second endpoint of the centerline is placed at $(1/2, 0, 0)$, with the cross-section such that $\mathbf{d}_1 = (1, 0, 0)$, $\mathbf{d}_2 = (0, 0, 1)$, and $\mathbf{d}_3 = (0, -1, 0)$. The solution configuration for these boundary conditions contains stretching, shear, bending, and torsion (see Fig. 4).

The material is modelled with the linear diagonal law (31) with parameters $A = (755, 755, 1963)$ and $K = (1.23, 1.23, 0.94)$. According to the theory of Clebsch and Kirchhoff (see, e.g., [9]), this corresponds to a rod with a circular cross-section of radius 0.05 length units, Young's modulus $E = 2.5 \cdot 10^5$ pressure units, and Poisson ratio $\nu = 0.3$. To avoid the phenomenon of locking (i.e., a bad approximation property of the discrete problem for coarse grids [4]), we follow Simo and Vu-Quoc [16] in using a selective integration scheme. For the planar case, Noor and Peters [12] showed this to be equivalent to a mixed discretization.

Convergence of the Solver Let $\mathcal{G}_n$ be a uniform grid on $[0, 1]$ with n vertices. We set up the Riemannian trust-region algorithm of the previous chapter using the maximum norm (34) for the definition of the trust region. For the inner solver we use a monotone multigrid method, which is a descent method with guaranteed multigrid convergence for convex quadratic problems [10, 13]. The inner problems are solved to a precision of 10^{-13} by tracking the H^1-norm of the relative corrections. The initial trust-region has a radius of 1 and the parameters η_1 and η_2 are set to 0.01 and 0.9, respectively. The scaling parameter α in the trust-region norm is set to 1.

To measure the convergence speed we first compute a reference solution φ^* by letting the solver iterate until the maximum norm of the correction $\|\exp_{\varphi_\nu}^{-1} \varphi_{\nu+1}\|_\infty$ drops below 10^{-12}. We then compute the Hesse matrix H^* of the lifted energy functional $\hat{\jmath}_*$ at the last iterate φ^*. Assuming φ^* to be close to a minimum of $\bar{\jmath}$ we get convexity of $\hat{\jmath}_*$ and hence H^* is positive definite. It therefore creates an energy norm on $T_{\varphi^*}\mathrm{SE}(3)^n$ which we denote by $\|\cdot\|_{H^*}$. Revisiting now the iteration history $\varphi_0, \ldots, \varphi^*$ we transport each φ_ν onto $T_{\varphi^*}\mathrm{SE}(3)^n$ using the inverse exponential map at φ^* and define the error of

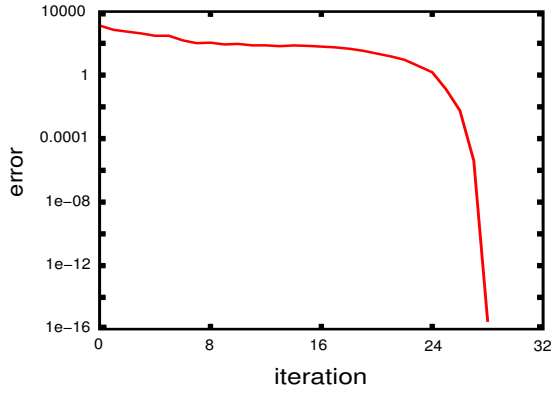

Figure 5: Error e_ν per iteration ν for a grid consisting of 4096 elements.

levels	2	3	4	5	6	7	8	9	10	11	12
elements	4	8	16	32	64	128	256	512	1024	2048	4096
overall it.	16	14	25	19	24	26	19	29	34	30	30
unsuccessful it.	2	1	2	1	3	4	2	3	5	1	1

Table 1: Number of overall iterations and unsuccessful iterations of the trust-region solver per grid size.

φ_ν as

$$e_\nu = \|\exp_{\varphi^*}^{-1} \varphi_\nu\|_{H^*}.$$

We first concentrate on trust-region convergence on a single grid. From the general theory for Riemannian trust-region methods we expect global convergence and local convergence at least close to quadratic. Fig. 5 shows the error per iteration on a grid of 4096 elements. The initial iterate is the unstressed reference configuration where the rod is straight along the z-axis, and the load is applied in a single step. One can see good global convergence in spite of the fairly remote starting iterate. The sharp drop starting around the 24th iteration confirms the predictions concerning fast local convergence.

Next we investigate the behavior of the convergence with respect to grid size. In analogy to [18] one would hope for asymptotically grid-independent convergence. Starting from a one-level grid with two elements of equal size we used uniform refinement to create a set of test grids. These grids have between two and twelve levels and correspondingly the range of element numbers goes from four to 4096. We ran the same problem as in the previous paragraph on each of these grids. Table 1 shows the number of trust-region iterations. They appear to be bounded from above, marking another desirable property of the algorithm.

Convergence of the Discretization In a second numerical experiment we measure the order of convergence of the discretization error. We get numerical evidence that the geodesic finite element solution converges optimally to a continuous solution, even though this has not been established theoretically yet.

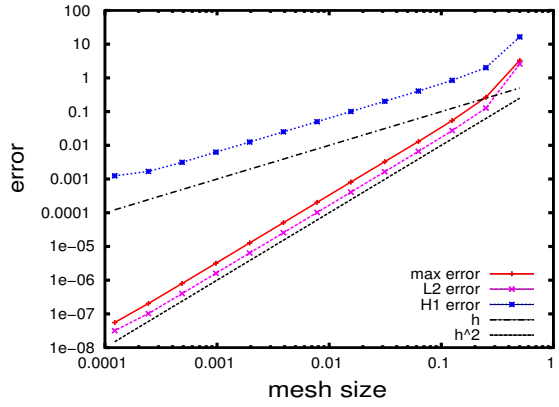

Figure 6: Measured discretization error as a function of the grid size h.

We consider the same problem setting as above and begin by computing a solution φ^* on a grid $\mathcal{G}_J$ consisting of $n^J = 2^{16} + 1 = 65\,537$ evenly-space vertices. This solution φ^* will be our reference solution. We then compute solutions φ^i, $0 < i < 16$ on grids consisting of $2^i + 1$ evenly-spaced vertices. To allow comparison between solutions in an algebraic setting, we interpolate the coarse solutions φ^i on the finest grid $\mathcal{G}_J$. Note that this does not lead to errors, as the geodesic finite element spaces are nested if the corresponding grids are. In an abuse of notation the interpolated solutions will again be denoted by φ^i. The errors with respect to the reference solution φ^* are then computed in three norms:

- The geodesic maximum norm

$$\|\varphi^i - \varphi^*\|_\infty = \max_{v_j \in \mathcal{G}_J} \operatorname{dist}\big(\varphi^i(v_j), \varphi^*(v_j)\big),$$

- the L^2-norm

$$\|\varphi^i - \varphi^*\|_{L^2} = \langle \delta^i, M_6 \delta^i \rangle_{T_{\varphi^*}\mathrm{SE}(3)^{n^J}},$$

  where $\delta^i = \exp^{-1}((\varphi^i)^{-1}\varphi^*) \in T_{\varphi^*}\mathrm{SE}(3)^{n^J}$ and

$$M_6 \in \mathbb{R}^{6n \times 6n}, \qquad (M_6)_{ij} = \mathrm{Id}_{6\times 6} \int_{[0,l]} \psi_i \psi_j \, ds$$

  is the vector-valued mass matrix on $T_{\varphi^*}\mathrm{SE}(3)^{n^J} \simeq \mathbb{R}^{n^J \times 6}$;

- the H^1-seminorm

$$\|\varphi^i - \varphi^*\|_{H^1} = \langle \delta^i, S_6 \delta^i \rangle_{T_{\varphi^*}\mathrm{SE}(3)^{n^J}},$$

  with δ^i as above and

$$S_6 \in \mathbb{R}^{6n \times 6n}, \qquad (S_6)_{ij} = \mathrm{Id}_{6\times 6} \int_{[0,l]} \psi_i' \psi_j' \, ds$$

  the stiffness matrix of the Laplace problem.

The results can be seen in Fig. 6. Both the maximum norm and the L^2 error decrease quadratically, whereas the H^1-seminorm decreases linearly as a function of the mesh size. This is optimal for a first-order method.

Acknowledgment

The author would like to thank Wolfgang Müller and Christian Wieners from the University of Karlsruhe for the interesting discussions.

References

[1] P.-A. Absil, R. Mahony, and R. Sepulchre. *Optimization Algorithms on Matrix Manifolds*. Princeton University Press, 2008.

[2] S. S. Antman. *Nonlinear problems of elasticity*, volume 107 of *Applied mathematical sciences*. Springer Verlag, Berlin, 1991.

[3] F. Bethuel. The approximation problem for Sobolev maps between two manifolds. *Acta Math.*, 167:153–206, 1991.

[4] D. Braess. *Finite Elemente*. Springer Verlag, 3rd edition, 2002.

[5] A. Conn, N. Gould, and P. Toint. *Trust-Region Methods*. SIAM, 2000.

[6] M. Crisfield and G. Jelenić. Objectivity of strain measures in the geometrically exact three-dimensional beam theory and its finite-element implementation. *Proc. R. Soc. Lond. A*, 455:1125–1147, 1999.

[7] D. J. Dichmann. *Hamiltonian Dynamics of a Spatial Elastica and the Stability of Solitary Waves*. PhD thesis, University of Maryland, 1994.

[8] M. do Carmo. *Riemannian Geometry*. Birkhäuser, 1992.

[9] S. Kehrbaum. *Hamiltonian Formulations of the Equilibrium Conditions Governing Elastic Rods: Qualitative Analysis and Effective Properties*. PhD thesis, University of Maryland, 1997.

[10] R. Kornhuber. *Adaptive Monotone Multigrid Methods for Nonlinear Variational Problems*. B.G. Teubner, 1997.

[11] J. Nash. The imbedding problem for Riemannian manifolds. *Ann. of Math.*, 63(1):20–63, 1956.

[12] A. Noor and J. Peters. Mixed models and reduced/selective integration displacement models for nonlinear analysis of curved beams. *Int. J. Numer. Methods Eng.*, 17:615–631, 1981.

[13] O. Sander. *Multidimensional Coupling in a Human Knee Model*. PhD thesis, Freie Universität Berlin, 2008.

[14] C. Sansour and W. Wagner. Multiplicative updating of the rotation tensor in the finite element analysis of rods and shells — a path independent approach. Technical Report 4, Universität Karlsruhe, Institut für Baustatik, 2002.

[15] T. Seidman and P. Wolfe. Equilibrium states of an elastic conducting rod in a magnetic field. *Arch. Rational Mech. Anal.*, 102(4):307–329, 1988.

[16] J. Simo and L. Vu-Quoc. A three-dimensional finite-strain rod model. Part II: Computational aspects. *Comput. Methods Appl. Mech. Engrg.*, 58 (1):79–116, 1986.

[17] M. Spivak. *Comprehensive Introduction to Differential Geometry*. Publish or Perish Inc., 1970.

[18] M. Weiser, A. Schiela, and P. Deuflhard. Asymptotic mesh independence of Newton's method revisited. 42(5):1830–1845, 2005.